THREE-DIMENSIONAL MODELING OF SEDIMENT TRANSPORT IN THE PEARL RIVER ESTUARY

C.H. Wang[1], Onyx W.H. Wai[2] and C.H. Hu[3]

ABSTRACT

A three-dimensional baroclinic model of 9-node quadrilateral elements with 2nd order accuracy for hydrodynamics and cohesive sediment transport is developed in this paper. The operator-splitting scheme is introduced to solve the governing equations: solving the horizontal advection term by the Eulerian-Lagrangian method, using the Finite Element Method for horizontal diffusion terms and the Finite Differential Method is applied for the vertical diffusion terms. The Mellor-Yamada level 2.5 turbulence closure sub-model is coupled to offer more reasonable vertical eddy viscosity.

The model was applied to simulate the 3D suspended sediment transport in the Pearl River Estuary under the action of two kinds of tidal types covering a spring tide and a neap tide in the wet season (July 1998). The computational domain of this simulation covers eight outlets, from which freshwater discharges to the Pearl River Estuary. The model is validated with the field data of tidal levels, tidal flows, salinities and suspended sediment concentrations. The numerical results of the proposed approach are in good agreement with the field data, generally. In addition, based on the simulated results, some physical phenomena, such as salinity intrusion, turbidity maximum in the Pearl River Estuary are discussed briefly.

1. INTRODUCTION

Cohesive sediment transport processes play a vital role in many aspects of marine environment and coastal engineering. Although, the estuarine environment is very complex, where the interaction of input fresh-water, tidal currents, waves, winds, Coriolis force, and even surges should be considered, and even the cohesive fine sediment characteristics of deposition and resuspension processes, flocculation and deflocculation, bed consolidation and so on, have not been known very well, there was considerable effort undertaken in recent years to develop and apply numerical models to predict coastal and estuarine sediment transport. For example, O'Connor and Nicholson (1988) provided a fully 3D model, including a fluid-mud transport model, flocculation and consolidation. Katopodi and Ribberink (1992) reported a quasi-3D model for suspended sediment transport based on an

[1] Senior Engineer, Department of sedimentation Engineering, China Institute of Water Resources and Hydropower Research, 20 West Chegongzhuang Rd., P.O. Box 366, Beijing 100044, China P.R.. Phone: 86-10-68786627 Fax: 86-10-68411174 Email: chwang@iwhr.com
[2] Associate Professor, Department of Civil and Structural Engineering, The Hong Kong Polytechnic University, Hung Hom, Kowloon, Hong Kong. Phone: 852-2766-6025 Fax: 852-2334-6389 Email: ceonyx@polyu.edu.hk
[3] Professor & Secretary-General, International Research and Training Center on Erosion and Sedimentation, 20 West Chegongzhuang Rd., P.O. Box 366, Beijing 100044, China P.R.. Phone: 86-10-68413372 Fax: 86-10-68411174 Email: chhu@iwhr.com

asymptotic solution of the convection-diffusion equation for currents and waves. Briand and Kamphuis (1993) gave a detailed approach to sediment transport calculations, in which quasi-3D velocities and local vertical distribution of suspended sediment concentrations were combined. A fully-3D finite difference baroclinic model system for hydrodynamics and fine suspended cohesive sediment transport was described by Cancino and Neves (1999). A refined three-dimensional layer-integrated model to predict salt and cohesive sediment transport in estuarine waters was proposed by Wu and Falconer (2000).

The Pearl River Estuary (PRE), also called Lingding Bay, is located in the east of the Pearl River Delta and connecting to the South China Sea, several developed cities including Hong Kong, Macau, Guangzhou and Shenzhen stand here. It is a bell-shaped estuary along direction of NNW-SSE (see Figure 1). For the need of economic developing, lots of hydro engineering are in construction, which demands the study of hydrodynamics and sediment transport. Xu et al. (1985) analyzed the tidal currents, residual flows, salt intrusion and sediment patterns in the PRE based on the numerous measurement data. Tian (1986) and Wai et al. (2004) discussed the existence and formation mechanism of turbidity maximum (TM). Wang et al. (2001) studied the characteristics of sediment transport by a vertical integrated 2-D model, and Xu and Lu (2003) developed a 2-D numerical model in body-fitted coordinate system to study the non-equilibrium non-uniform sediment transport in the Lingding bay. Furthermore, in order to reveal the real flow structure and sediment concentration in a water column, three-dimensional models have also been used to study the sediment transport in the PRE (Chen et al., 1999; Li et al., 2003). However, most of these models exclude the salinity and do not consider the baroclinic term, which is an important source force to drive the salt water landward. For the study of turbidity maximum, a typical phenomenon in partial-mixed estuaries, a more accurate turbulence closure is also necessary.

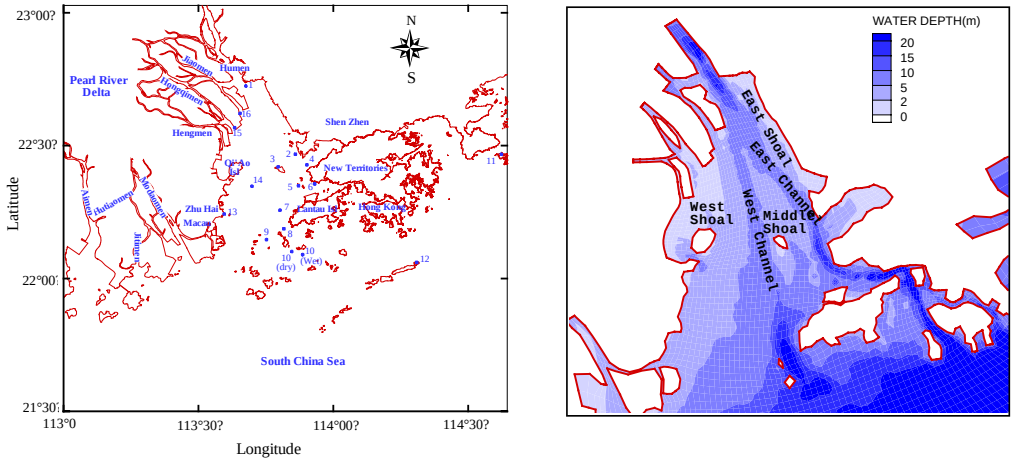

Figure 1 Bathymetry, measurement stations in the PRE.

2. MODEL DESCRIPTION

2.1 Governing Equations

The Navier-Stokes equations under the assumption of hydrostatic pressure and Boussinesq approximation after Reynolds averaging in the Cartesian coordinate are used in this model; due to the salinity gradient in horizontal direction, the baroclinic term is also taken into account.

Continuity equation of flow is

$$\frac{\partial u}{\partial x}+\frac{\partial v}{\partial y}+\frac{\partial w}{\partial z}=0 \tag{1}$$

Momentum equations of flow are

$$\frac{\partial u}{\partial t}+u\frac{\partial u}{\partial x}+v\frac{\partial u}{\partial y}+w\frac{\partial u}{\partial z}=-g\frac{\partial \zeta}{\partial x}-\frac{g}{\rho_0}\frac{\partial}{\partial x}\left(\int_z^\zeta \rho' dz'\right)+\frac{\partial}{\partial x}\left(\varepsilon_h\frac{\partial u}{\partial x}\right)+\frac{\partial}{\partial y}\left(\varepsilon_h\frac{\partial u}{\partial y}\right)+\frac{\partial}{\partial z}\left(\varepsilon_z\frac{\partial u}{\partial z}\right)+fv \tag{2}$$

$$\frac{\partial v}{\partial t}+u\frac{\partial v}{\partial x}+v\frac{\partial v}{\partial y}+w\frac{\partial v}{\partial z}=-g\frac{\partial \zeta}{\partial y}-\frac{g}{\rho_0}\frac{\partial}{\partial y}\left(\int_z^\zeta \rho' dz'\right)+\frac{\partial}{\partial x}\left(\varepsilon_h\frac{\partial v}{\partial x}\right)+\frac{\partial}{\partial y}\left(\varepsilon_h\frac{\partial v}{\partial y}\right)+\frac{\partial}{\partial z}\left(\varepsilon_z\frac{\partial v}{\partial z}\right)-fu \tag{3}$$

$$\frac{\partial P}{\partial z}=-\rho g \tag{4}$$

The conservation equation of salinity is

$$\frac{\partial s}{\partial t}+u\frac{\partial s}{\partial x}+v\frac{\partial s}{\partial y}+w\frac{\partial s}{\partial z}=\frac{\partial}{\partial x}\left(\varepsilon_{s,h}\frac{\partial s}{\partial x}\right)+\frac{\partial}{\partial y}\left(\varepsilon_{s,h}\frac{\partial s}{\partial y}\right)+\frac{\partial}{\partial z}\left(\varepsilon_{s,z}\frac{\partial s}{\partial z}\right) \tag{5}$$

The governing equation for water-sediment mixture of low concentrations in Cartesian coordinate system is written as follows:

$$\frac{\partial c}{\partial t}+u\frac{\partial c}{\partial x}+v\frac{\partial c}{\partial y}+w\frac{\partial c}{\partial z}-\frac{\partial \omega_s}{\partial z}=\frac{\partial}{\partial x}\left(\varepsilon_{s,h}\frac{\partial c}{\partial x}\right)+\frac{\partial}{\partial y}\left(\varepsilon_{s,h}\frac{\partial c}{\partial y}\right)+\frac{\partial}{\partial z}\left(\varepsilon_{s,z}\frac{\partial c}{\partial z}\right) \tag{6}$$

where t is time; u, v and w are the current velocity components in the x, y and z directions, respectively , in the Cartesian coordinate system; ζ is the tidal level; z is the vertical coordinate increasing upward with z =0 located at the undisturbed sea surface, and positive upward, z' is an independent variable; ρ is the density of clear sea water, ρ_0 is the constant reference density, ρ' is the local variation from the reference density; g is the gravitational acceleration; f is the Coriolis parameter; s is the salinity; c is the suspended sediment concentration; ω_s is the settling velocity of sediment particles; ε_h and ε_z are the eddy viscosity of turbulent flow in the horizontal and vertical directions, respectively; and $\varepsilon_{s,h}$ and $\varepsilon_{s,z}$ are the horizontal and vertical diffusivities of scalars, respectively.

The Mellor-Yamada Level 2.5 turbulence closure model (Mellor and Yamada, 1982) together with a prognostic equation (Mellor et al., 1998) for the turbulent macroscale is adopted to calculate the vertical eddy viscosity and diffusivity. The Mellor-Yamada Level 2.5 turbulence closure uses two partial differential equations to compute the turbulent kinetic energy (q^2) and a turbulent macroscale (l).

The equation for the turbulent kinetic energy is

$$\frac{\partial q^2}{\partial t}+u\frac{\partial q^2}{\partial x}+v\frac{\partial q^2}{\partial y}+w\frac{\partial q^2}{\partial z}=\frac{\partial}{\partial x}\left(\varepsilon_q\frac{\partial q^2}{\partial x}\right)+\frac{\partial}{\partial y}\left(\varepsilon_q\frac{\partial q^2}{\partial y}\right)+\frac{\partial}{\partial z}\left(\varepsilon_q\frac{\partial q^2}{\partial z}\right)+2\left[P_s+P_b-\frac{q^3}{B_1 l}\right] \tag{7}$$

and the turbulent macroscale is

$$\frac{\partial q^2 l}{\partial t}+u\frac{\partial q^2 l}{\partial x}+v\frac{\partial q^2 l}{\partial y}+w\frac{\partial q^2 l}{\partial z}=\frac{\partial}{\partial x}\left(\varepsilon_q\frac{\partial q^2 l}{\partial x}\right)+\frac{\partial}{\partial y}\left(\varepsilon_q\frac{\partial q^2 l}{\partial y}\right)+\frac{\partial}{\partial z}\left(\varepsilon_q\frac{\partial q^2 l}{\partial z}\right)$$
$$+lE_1\left[P_s+P_b\right]+lE_1E_3\frac{g}{\rho_0}\left(\frac{\partial\rho}{\partial z}-\frac{1}{v_s{}^2}\frac{\partial p}{\partial z}\right)-\frac{q^3}{B_1}\left[1+E_2\left(\frac{l}{\kappa L}\right)^2\right] \tag{8}$$

where the shear production $P_s=\varepsilon_z\left(\frac{\partial u}{\partial z}\right)^2+\varepsilon_z\left(\frac{\partial v}{\partial z}\right)^2$; the buoyant production $P_b=\frac{g}{\rho_0}\varepsilon_{s,z}\frac{\partial\rho}{\partial z}$, $q^3/B_1 l$ is the turbulent dissipation; $L=\left[(\zeta-z)^{-1}+(H-z)^{-1}\right]$; $\varepsilon_q = qlS_q$ is the eddy diffusion coefficient for turbulence energy; p is the water pressure; v_s is the sound speed; and k is the von Karman constant. The last term in the equation accounts for the effects of solid walls and the free surfaces on the length scale.

The vertical eddy viscosity and diffusion coefficients ε_z and $\varepsilon_{s,z}$ are defined according to $\varepsilon_z = qlS_z$ and $\varepsilon_{s,z} = qlS_s$. The coefficients S_z and S_s are stability functions related to Richardson number, and given by

$$S_z=\frac{A_2\left(1-6A_1/B_1\right)}{1-\left(3A_2B_2+18A_1A_2\right)G_H},\quad S_{s,z}=\frac{A_1\left(1-3C_1-6A_1/B_1\right)+S_z\left(18A_1^2+9A_1A_2\right)G_H}{1-9A_1A_2G_H} \tag{9}$$

here $G_H=-\frac{l^2}{q^2}\frac{g}{\rho_0}\left(\frac{\partial\rho}{\partial z}-\frac{1}{v_s^2}\frac{\partial p}{\partial z}\right)$, the constants use in these equations are A_1=0.92, A_2=0.74, $B_1=16.6$, $B_2=10.1$, C_1=0.08, $E_1=1.8$, E_2=1.33, E_3=0.25-1.0, S_q=0.2 (Rodi, 1993).

2.2 Boundary Conditions

The open boundary conditions of flow, salinity and sediment concentration are usually prescribed by using field data, if known. The fluxes are set to zero on the close boundaries, generally. The boundary conditions of flow at the free water surface and seabed specify the stresses and vertical velocity, which can be expressed by

$$\rho\varepsilon_z\left(\frac{\partial u}{\partial x},\frac{\partial v}{\partial x}\right)=\begin{cases}\left(\tau_{s,x},\tau_{s,y}\right) & \textit{at water surface}\\ \left(\tau_{b,x},\tau_{b,y}\right) & \textit{at seabed}\end{cases} \tag{10}$$

$$w=\begin{cases}\dfrac{\partial\zeta}{\partial t}+u\dfrac{\partial\zeta}{\partial x}+v\dfrac{\partial\zeta}{\partial y} & \textit{at water surface}\\ -u\dfrac{\partial h}{\partial x}-v\dfrac{\partial h}{\partial y} & \textit{at seabed}\end{cases} \tag{11}$$

The boundary conditions of turbulence energy and macroscale applied at the water surface and bottom boundaries, respectively, are

$$q^2 = B_1^{2/3} u_*^2, \qquad q^2 l = 0 \tag{12}$$

and there is no exchange of salinity at both water surface and seabed. The flux of sediment at water surface is also set to zero. However, sediment flux at bottom denotes the sediment exchange between water column and the seabed, noted as q_s, is defined by the following expression.

$$q_s = \omega_s c + \varepsilon_{s,z} \frac{\partial c}{\partial z} \tag{13}$$

This expression represents the net flux of the sediment in the vertical direction, expressed as the difference of the downward sediment flux, $D = \omega_s c$, and the upward sediment flux, $E = -\varepsilon_{s,z} \frac{\partial c}{\partial z}$. That is $q_s = D - E$. To avoid calculating the cohesive sediment concentration at bottom directly, the net flux of sediment at seabed is defined as follows:

$$q_s = \begin{cases} \alpha_s \omega_s (\bar{c} - c_a) & (\bar{c} > c_a) \\ \alpha_s \omega_s (\bar{c} - c_a) & (\bar{c} \le c_a \ and \ \tau_b > \tau_{b,cr}) \\ 0 & (\bar{c} \le c_a \ and \ \tau_b \le \tau_{b,cr}) \end{cases} \tag{15}$$

where α_s is the probability of the sediment settling in the range of 0 to1; c_a is the vertical-averaged sediment carrying capacity; $\bar{c}$ is the vertical sediment averaged concentration; τ_b is the bed shear stress; $\tau_{b,cr}$ is the incipient bed shear stress.

2.3 Numerical Scheme

The σ-coordinate transformation is applied to transform temporally and spatially and an efficient splitting method, which was developed by Lu and Wai (1998) and has been confirmed as a stable and effective approach by Chen et al. (1999) and Jiang (2003), is used to partition the complicated physical characteristics into several simple procedures. The hydrodynamic equations and mass conservation and transport equations are solved in three sub-steps: In the first step, the advection term and Coriolis force term in momentum equations, pure advective terms of scalar variables of salinity conservation, sediment transport and kinetic energy of turbulence and macroscale of turbulent eddy are solved by the Eulerian-Lagrangian method; In the second sub-step, the horizontal diffusion terms are considered, and is approximated by the implicit finite element method in each layer; The vertical diffusion terms and pressure terms in the momentum equations, the vertical dispersion terms and source-sink terms in the scalar transport equations are performed in the third sub-step, where the equations are approximated by the implicit finite differential method, and is solved by using the double sweep method in each column efficiently.

3. MODEL APPLICATION

3.1 Field Measurement

In July 1998, a hydrographic and water quality survey during the wet season (July) was carried out by the Hong Kong Civil Engineering Department. The location of the monitoring stations is shown

in Figure 1. The hydrographic survey consists of a 30-day continuous survey on water level variation at 5 specified stations from June 20 to July 20, a 15-day fixed station continuous measurement on currents and depths at specified stations from July 1 to 16, a 28-hour ship-based measurement on profiles of CTD and a 28-hour simultaneous water quality sampling at the specified stations and laboratory testing on a variety of water quality parameters during neap tides (July 4 to 5) and spring tides (July 9 to 10).

The marine water was monitored for the specific parameters including suspended solids, temperature, salinity, heavy metal, and so on. All water quality samplings were sampled at least 72 hours after commencement of fixed station survey. Each sampling spans 28 hours at an interval of 3 to 3.5 hours, giving a total of 8 samples for each sampling station. For in-situ measurements, hydrographic parameters were made at 1 m interval from surface to sea bottom. For on-situ measurements, water samples were collected at 5 depths (at equal vertical interval from surface to seabed). In addition, hourly measurement of water depth, current speed and direction were carried out at specified stations.

3.2 Modeling Parameters

To simulate tidal current, salinity intrusion and sediment transport in the PRE, a large coastal area, covering entire PRE, is selected to be the computational domain, extending to the water depth contour of 70 m in the South China Sea. The domain is divided into 1404 nine-node elements and the total nodes are 6036. The computational area is of 203 km × 188 km in size with an available water area of about 18500 km^2, the area of each element is from 0.3 km^2 in the Hong Kong Waters to 63 km^2 near open sea boundary. The water column is divided into 10 layers equally from seabed to water surface at each node.

The model is driven by the seasonal-mean flow rates at the eight river outlets, and four harmonic tidal components of M2, S2, O1 and K1 at the open sea boundaries. Corresponding seasonal-mean sediment concentration is set at the outlets. Salinity at the open sea boundary is set to 33 ppt during the wet season.

The model ran from 0:00 July 1 to 0:00 July 11, each simulation duration spans a spring tide and a neap tide. A five-day simulation was done beforehand as the background initial conditions for validation. The time step of this simulation is 180 s.

3.3 Model Calibration

The model was validated by tidal levels, current (speed and direction) and flow pattern, salinity profiles and sediment concentrations at specified stations.

The comparison of the computed and observed tidal levels at station 1, 3, 12 and 13 during a spring tide in the wet season is shown in Figure 2. Generally, considering only four tidal harmonic components driving the model, both the computed amplitudes and phases of tidal levels are deemed in good agreement with the observed ones. The mean errors of tidal levels to the observed ones are less than 0.15 m. Tidal errors at river outlets are a little larger than that at other stations, that maybe possibly caused by the inconsistent of boundary conditions with the real processes of flow rates. Due to the bottom friction and the restriction of topography, the tidal ranges increase from the open sea to Humen when tidal current propagates upstream, the input freshwater will affect not only the tidal currents, but also the tidal levels consequentially, especially near the outlets.

Tidal currents in the PRE are not only affected by the tides from the open sea, but also heavily affected by the strong runoff discharging from the Pearl River through eight outlets. Consequentially, the tidal flow is lack of balance between flooding and ebbing. Generally, the velocity during ebbing is larger than flooding, and the duration of ebbing is longer than flooding (Xu, et al., 1985). The model compared the velocity and its flow direction (clockwise from north) at

stations 6 and 8 with observed ones, shown in Figure 3. Stations 6 and 8 locate at the end of the East Channel and West Channel, respectively. It can be seen that both the magnitude of computed velocity and its direction at different layers are in good agreement with the measurements at each station, which means the model can simulate tidal currents well. Stations 6 and 8 locate far away from the outlets, the effect of input freshwater on the current is weaker, the duration of flooding and ebbing flow shows symmetric at a certain extent, the main flow go back and forth along their own deep channels, the model gets well results of these flow characters.

Figure 4 shows the time series of computed and measured salinity from the bottom layer, middle layer to the surface layer at Station 6 and 8 during a spring tide (July 9th to 10th) in the wet season (July, 1998). It can be seen that the computed salinity at different layers are in agreement with the measured ones at different stations, generally. It implies that not only the model can be used to simulate the advection and diffusion of conservative mass reasonably, but also the boundary conditions set at the Pearl River outlets correspond with the real situations basically.

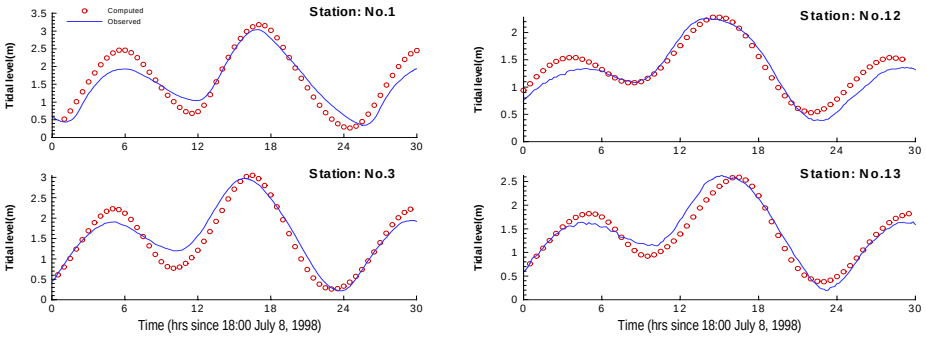

Figure 2 Comparison of computed tidal levels with observed ones.

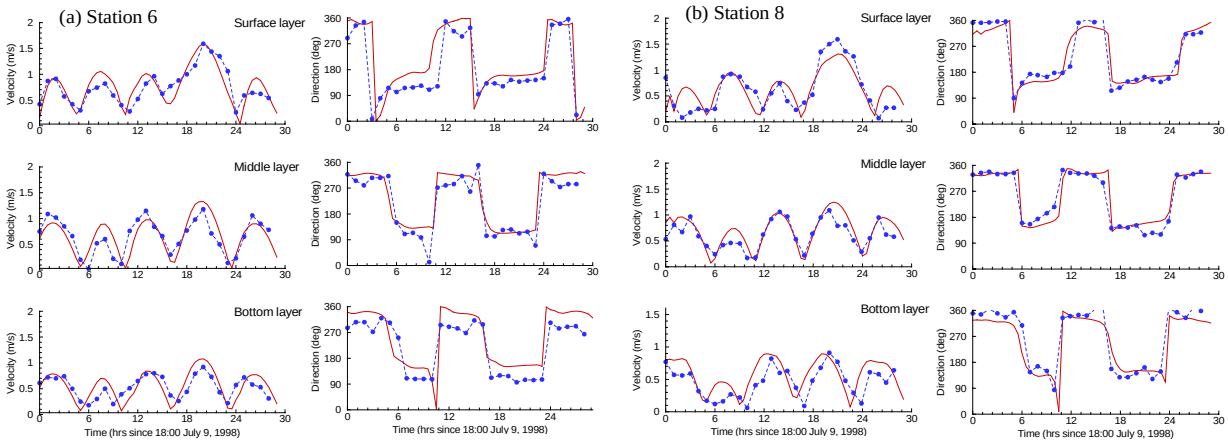

Figure 3 Comparison of computed flow velocities and directions with measurements at Station 6 and 8.

Figure 5 compared the profiles of computed suspended sediment concentrations with measurements at Station 6 and 8 during a spring tide (July 9th to 10th) in the wet season (July, 1998). The computed sediment concentrations are in good agreement with measurements generally; the model results reveal the resuspension processes during tidal flooding and ebbing, and the deposition processes during tidal slack periods. During flooding and ebbing, the sediment particles are resuspended from the seabed, the sediment concentration near bottom increases quickly from near 0

to 30-50 mg/l at these two stations, and the differences of sediment concentration between the bottom layer and surface layer are also simulated well by the model.

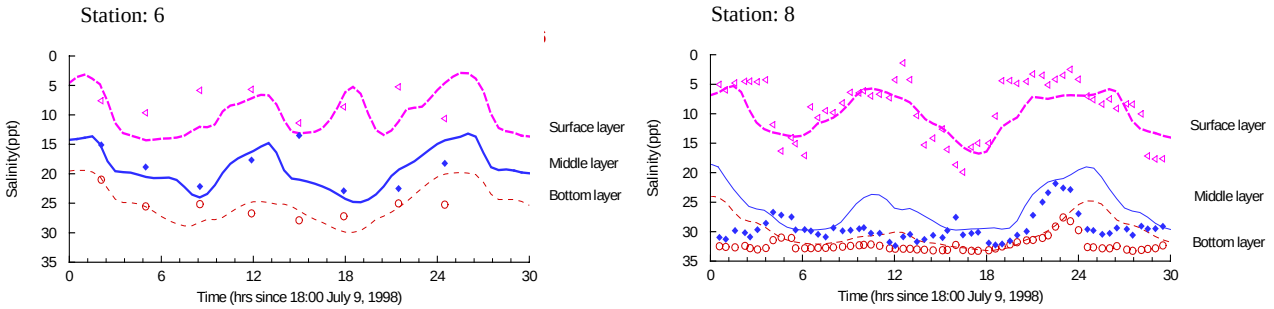

Figure 4 Comparison of computed salinities with measurements at Station 6 and 8.

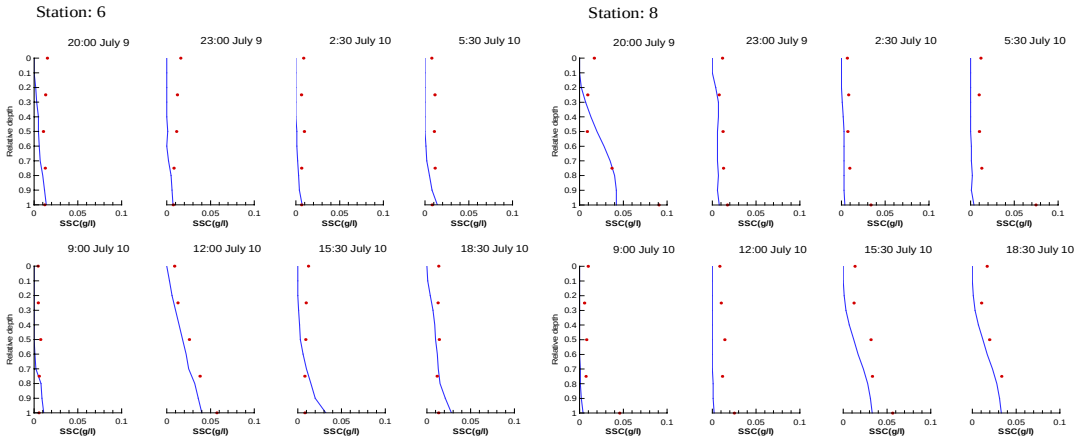

Figure 5 Comparison of the profiles of computed suspended sediment concentration with measurements at Station 6 and 8.

3.4 Sediment Transport in the PRE

Due to the existence of multi Pearl River outlets, sediment transport in the PRE is very complex; it is not only heavily affected by the input from the Pearl River, but also by tidal pumping, local resuspension, and flocculation and so forth. Figure 6 shows the suspended sediment concentration distribution at high slack, ebbing and low slack during a spring tide. Generally, the suspended sediment concentrations in channels are less than that on shoals, and the concentration in the East Channel is less than that in the West Channel, because the latter is much heavier affected by the input from the west outlets, and the sediment concentration near Humen is lower. In Hong Kong Waters, sediment concentration is small. Sediment particles depositing at high slack period will be resuspended during tidal ebbing, when a belt of high sediment concentration can be found from the Hongqimen to the east of Qi'ao island, sediment particles will go through the main channels, and reach the Hong Kong waters.

To study the relationship of residual flow, salt-water intrusion and the sediment concentration, the calculated results over tidal cycles are averaged. Figure 7 shows the stagnant point, salt wedge and turbidity maximum (TM) along the main channels, we can see the gravitational circulation flow structure, net flow flux flows seaward at the upper layer, and with net flow landward at the lower layer, the stagnant points locate at the end of the sand bars. It is caused by the stratification of flow due to the intrusion of salt water, high stratification along the West Channel due to the heavier input

freshwater, weak stratification along the East Channel due to the dominant tidal flow. The gravitational circulation and tidal pumping (Wang et al. 2004) cause the turbidity maximum in the PRE, Figure 7 also shows the computed TMs in the PRE, their locations correspond with the stagnant points and the heads of intrusion salt water. Particularly, due to the complicated bathymetry in the PRE, two TMs can be found in the West Channel, the second one, downstream of the West Channel, is in accord with the general character of TM in a partial-mixed estuary, the upstream TM is caused by the sediment particles from western outlets.

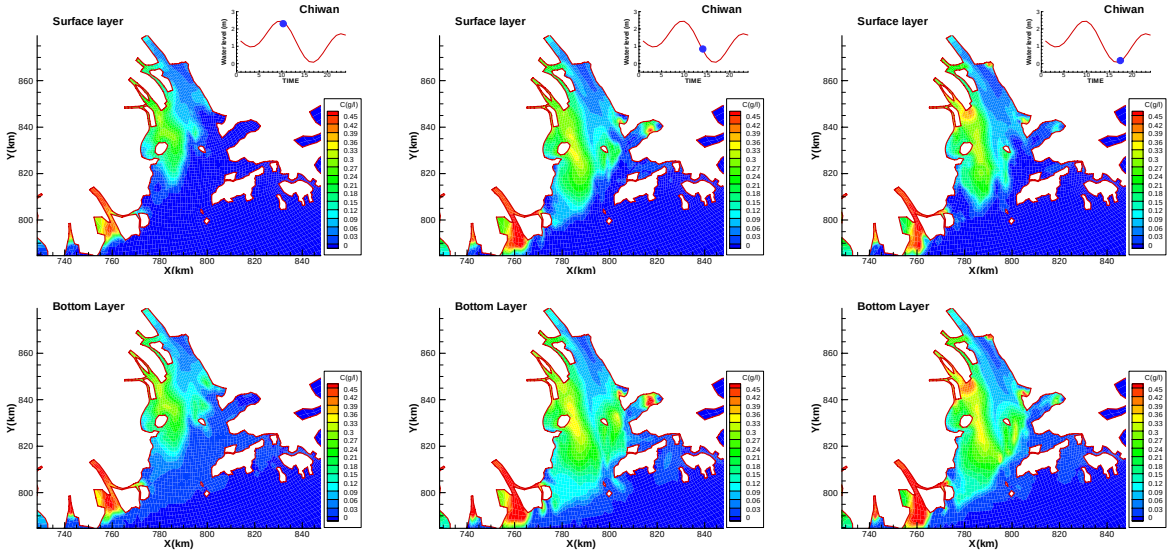

Figure 6 Suspended sediment concentration patterns

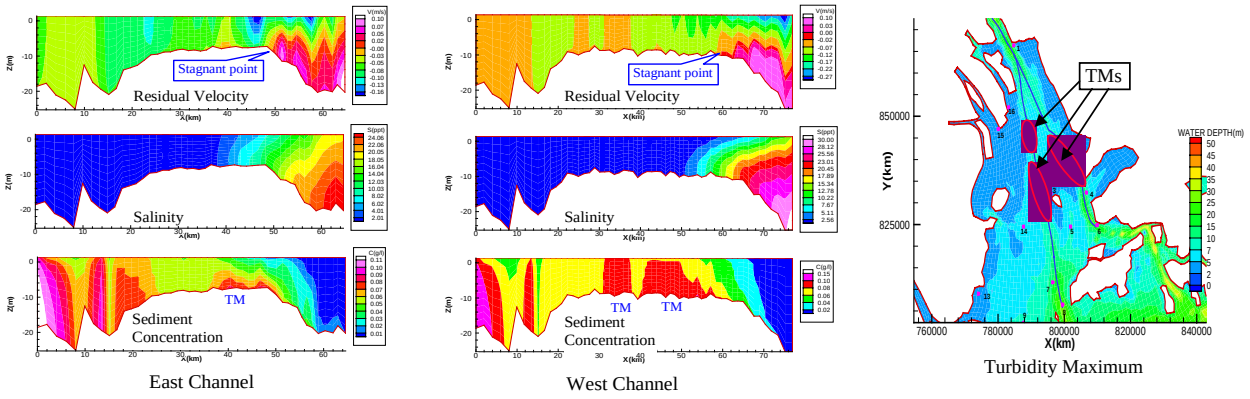

Figure 7 Stagnant point, salt wedge and turbidity maximum (MT) along main channels

4. CONCLUSIONS

In this paper, a three-dimensional hydrodynamics and sediment mass transport model is developed and applied to study the sediment transport in the Pearl River Estuary (PRE). Based on the above studies, the following conclusions can be drawn primarily:

(1) The operator-splitting method applied to approximate and resolve the governing equations is stable and effective. The model is improved in accuracy by considering the baroclinic term and coupling the turbulence closure of Mellor-Yamada level 2.5.

(2) The model was validated by measurement data, carried out during a spring tide in July 1998. The computed results of tidal level, flow velocity, salinity and sediment concentration are in good agreement with the measurements, generally.

(3) The relationships of net flow flux, saltwater intrusion and the turbidity maximum in the PRE are analyzed. Gravitational circulation exists along the main channels, and the stagnant points locate at the end of the sand bars, their locations are in accord with typical turbidity maximums. Due to the complex topography, the input sediment from the western river outlets can also produce the particular TMs.

ACKNOWLEDGEMENTS

The project was in part supported by The Hong Kong Polytechnic University/Internal Research Grant (grant number: G-V783) and by Research Grants Council, Hong Kong (grant number: PolyU 5038/98E). The Hong Kong Civil Engineering Department provides plentiful field data.

REFERENCES

Briand, M.H.G. and Kamphuis, J.W. (1993). "Sediment Transport in the Surf Zone: a Quasi 3-D Numerical model", Coastal Engineering, Vol. 20, pp. 135-166.

Cancino, L. and Neves, R. (1999). "Hydrodynamic and Sediment Suspension Modeling in Estuarine Systems Part I: Description of the Numerical Models." Journal of Marine Systems, Vol. 22, pp.105-116.

Chen Y., Wai W.H. Onyx, Li Y.S. and Lu Q.M., (1999). "Three-dimensional numerical modeling of cohesive sediment transport by tidal current in Pearl River Estuary". International Journal of Sediment Research, Vol. 14, No. 2, pp. 107-123.

Katopodi, I. and Ribberink, J.S. (1992). "Quasi-3D Modeling of Suspended Sediment Transport by Currents and Waves", Coastal Engineering, Vol. 18, pp. 83-110.

Li, M.G., SHI, Z. and Qin, C.R. (2003). "Three-dimensional Suspended Sediment Movement Simulation of the Lingding Bay", Shui Li Xue Bao, No. 4, pp. 51-57.

Lu, Q.M. and Wai, W.H. (1998). "An Efficient Operator Splitting Scheme for Three-dimensional Hydrodynamic Computations", International Journal for Numerical Methods in fluids, Vol. 26, pp. 771-789.

Jiang Y.W. (2003). Three-dimensional Numerical Modelling f Sediment and Heavy Metal Transport in Surface Waters, Ph.D Thesis of the Hong Kong Polytechnic University.

Mellor, G. L., and Yamada, T. (1982). "Development of A Turbulence Closure Model for Geophysical Fluid Problems", Reviews of Geophysics and Space Physics, Vol. 20, No. 4, pp. 851-85.

Mellor, G. L., Oey, L. Y. and Ezer, T. (1998). "Sigma Coordinate Pressure Gradient Errors And the Seamount Problem." Journal of Atmospheric and Oceanic Technology, Vol. 15, pp. 1122-1131.

O'Connor, B.A. and Nicholson, J.A. (1988). "Mud Transport Modeling", in Physical Processes in Estuaries, Springer-Verlag, pp. 532-544.

Rodi, W. (1993). Turbulence Models and Their Application in Hydraulics, IAHR Monograph Series, Third Edition, The Netherlands.

Tian, X.P. (1986). "A Study on Turbidity Maximum in Lingdingyang Estuary of the Pearl River". Tropic Oceanology, No. 5, pp. 27-35. (in Chinese)

Wai, W.H. Onyx, Wang, C.H. and Li, Y.S. (2004). "The Formation Mechanisms of Turbidity Maximum in the Pearl River Estuary, China", Marine Pollution Bulletin, 48, pp. 411-448.

Wang, C.H., Wai, W.H. and Li, Y.S. (2001). "Two-dimensional Characteristics of Hydrodynamics and Sediment Transport in the Pearl River Estuary", Proceedings of 29th IAHR Congress, Beijing, Vol. II, pp. 396-401.

Wang, J.M., Yu, G.Y. and Chen, Z.Y. (1992). "Numerical Simulation of Tidal Current in Lingding Bay in the Pearl River Estuary", ACTA Oceanologica Sinica, No. 14, pp. 26-34. (in Chinese)

Wu, Y. and Falconer, R.A. (2000). "A Mass Conservative 3-D Numerical Model for Predicting Solute Fluxes in Estuarine Waters", Advances in Water Resources, Vol. 23, pp. 531-543.

Xu, J.F. and Liu, J.Y. (2003). "2-D Numerical Modeling on Sediment Transport of Lingdingyang Sea Area in Zhujiang River Estuary", Shui Li Xue Bao, No. 7, pp. 16-21. (in Chinese)

Xu, J.L., Li, Y.X., Can, F.X. and Chen, Q.D. (1985). Evolution of Channels and Shoals in Lingding Sea, PRE, Ocean Press, Beijing. (in Chinese)